Biosensors and Bioelectronics 135 (2019) 30–35

Contents lists available at ScienceDirect

Biosensors and Bioelectronics

journal homepage: www.elsevier.com/locate/bios

Automated DNA hybridization transfer with movable super-paramagnetic microbeads in a microflow reactor

Robert Penchovsky

Department of Genetics, Faculty of Biology, Sofia University "St. Kliment Ohridski", 8 Dragan Tzankov Blvd., 1164, Sofia, Bulgaria

ARTICLE INFO

Keywords:
Microfluidics
Super-paramagnetic beads
DNA hybridization under flow conditions
DNA selection under isothermal conditions
Fluorescent DNA detection

ABSTRACT

An automated DNA hybridization transfer in a microflow reactor is demonstrated by moving paramagnetic beads between two spatially separate solutions with different pH values. The microbeads-based microfluidic platform is fully automated and programmable. It employs a robust chemical procedure for specific DNA hybridization transfer in microfluidic devices under isothermal conditions based on reversible pH alterations. The method takes advantage of high-speed DNA hybridization and denaturation on beads under flow conditions, high fidelity of DNA hybridization, and small sample volumes. The microfluidic platform presented is saleable and applicable to many areas of modern biotechnology such as DNA hybridization chip microarrays, molecular computation, on-chip selection of functional nucleic acids, high-throughput screening of chemical libraries for drug discovery, and DNA amplification and sequencing.

1. Introduction

Micro-and-nano-fluidics have been used for the development of various lab-on-a-chip platforms for many different applications in modern biotechnology. Such applications include real-time detection of gene expression (Yan et al., 2016), microRNA analysis (Shamsi et al., 2016), cyanobacteria identification (Olcer et al., 2015), single cell arrays (Zhao et al., 2016), DNA sequencing and SNP analyses (Penchovsky, 2013b), PCR-based amplification (Pekin and Taly, 2017), (Yu et al., 2017) virus detection (Na et al., 2018), and many others. Therefore, it is important to engineer various microfluidic devices that can be used as functional elements in building complex microfluidic platforms. Here we demonstrate the application of one microfluidic module for automated DNA selection by hybridization and denaturation on movable paramagnetic microbeads under isothermal conditions. We applied already established a chemical procedure for reversible pH alterations for multiple DNA selections on beads placed in cascade microchambers (Penchovsky and McCaskill, 2002) (Penchovsky, 2013b). Here, we employ different microfluidic design using switching paramagnetic beads between microchannels with hybridization or denaturation solutions. The method is fully automated, programmable, and reusable since the beads can be moved, immobilized with different DNA oligomers, and replaced automatically into the microreactor. It takes advantages of small reaction volume needed, fast DNA hybridization kinetics on beads under flow conditions, the instant DNA denaturation by NaCl under flow conditions (Penchovsky, 2013b). The approach is applicable to many biotechnological applications, including DNA detection, selection, and amplification. It can be integrated into complex microfluidic designs for various applications such as DNA/RNA computing (Penchovsky and Ackermann, 2003), (Penchovsky and Breaker, 2005), (Penchovsky, 2012), molecular diagnostics (Penchovsky, 2012), (Penchovsky, 2013b), selection of functional DNA molecules (Penchovsky, 2014), and drug discovery (Blount et al., 2006), (Penchovsky and Stoilova, 2013), (Penchovsky, 2013a), (Penchovsky and Traykovska, 2015). The application of DNA selection under isothermal conditions can allow us to integrate more selection modules on a single-wafer than that using a temperature gradient because silica is a very good thermo-conductor.

2. Materials and Methods

2.1. Synthetic DNA oligomers, DNA immobilization to super-paramagnetic beads, and PCR amplification

The deoxyoligonucleotides were obtained from IBA-NAPS (Göttingen, Germany). All of them were purified by HPLC. Carboxyl-coated PVA beads, diameter = 15 μm ± 3, with a high magnetic content (50%), were purchased from Chemagen (Baesweiler, Germany). The beads were essentially monodispersed. Amino-modified (5′-end) deoxyoligonucleotides at a concentration of 10 μM were immobilized to the carboxyl-coated beads in the presence of 50 mM EDAC (Ethylene Di Amid Carbodiimide), 100 mM MES buffer, pH 6.1, and 100 mM NaCl in

E-mail address: robert.penchovsky@hotmail.com.

https://doi.org/10.1016/j.bios.2019.04.014
Received 16 September 2018; Received in revised form 24 March 2019; Accepted 6 April 2019
Available online 11 April 2019
0956-5663/

a final volume of 200 µl at room temperature under shaking. The immobilization reaction results in the formation of a peptide bond between the 5′-end amino-group of the modified DNA oligomer and the carboxyl-group on the bead surface. The beads were moved from the left–hand part of the chamber to the right-hand part and backward applying a magnetic stand (IBS Magnet, Berlin, Germany) put onto the micro-reactor bottom. A NdFeB block magnet, 30 × 18 × 10 mm, produced of DIN type material, code 360/95. The magnet was placed on the bottom of the microreactor and moved by a small robotic arm guided by LabVIEW software (National Instruments, Austin, Texas).

The PCR experiments were performed by a gradient thermo-block LKB Quantarus Q Cycler. The amplification program started with an initial denaturation at 93 °C for 3 min followed by 28 cycles of denaturation at 93 °C for 30 s, annealing at 53 °C for 40 s and elongation at 72 °C for 30 s. The Taq polymerase was purchased from Qiagen (Hilden, Germany) and used in a concentration of 0,1 U/µl. The amplification reactions were carried out in a 1x incubation buffer in the presence of 1 µM sense primer, 0,5 µM antisense primer (capture probes – see Fig. 3B), 1 pM single-stranded DNA template and 250 µM dNTP mixture. The PCR products were analyzed on 4% agarose gel electrophoresis, in the presence of a 0.5x TBE buffer. The gels were stained in a 1x SYBR Green One dye (Molecular Probes, Eugene, OR). The gel pictures were obtained by a gel documentation system from ImageQuant300 (Applied Biosystems, USA).

2.2. Design and manufacturing of microflow reactors

The microflow reactor was photolithographically etched onto 100 mm silicon wafers using tetramethylammonium hydroxide (TMAH) and KOH at 80 °C using two masks etched to different depths. The first mask (Fig. 1B), producing the bead chamber, was etched to a depth of 10 µm. The second mask (Fig. 1C), representing the inlet (on the top) and outlet (on the bottom) channels, is etched to a depth of 75 µm and to a width of 180 µm. After this, the microreactor was sealed with anodically bonded 500 µm thick Pyrex (borosilicate) glass wafers. Ultrasonically drilled holes in the Pyrex wafers (distance between the holes 3.5 mm) were connected with capillary tubing (0.8 mm in diameter) using UV-hardening glues.

2.3. Fluorescence imaging setup

Fluorescence imaging of DNA/DNA hybridization on beads placed in microreactor chambers was performed using an inverted microscope model Axiovert 100 TV (Carl Zeiss, Jena, Germany). The microscope was connected to an argon-ion laser model 2080–15S (Spectra-Physics Lasers, Inc., CA) by an optical fiber. A homogeneous pool of light was created by the acoustic vibration of the optical fiber at 80 Hz with an arbitrary wave by a generator model 3312A (Hewlett-Packard, Palo Alto, CA). The images were detected by 12-bit CCD cameras (models CH250 or Quantix, from Photometrics, Tucson, AZ) connected to the microscope by a C-Mount adapter (Fig. S1). An emission filter opening at 540 nm and closing at 580 nm (Oriel Instruments, Stanford, CT) was employed. The images were obtained and analyzed by the PMIS image processing software (GKR Computer Consulting, Boulder, CO). In all flow experiments, the fluids were delivered to the microreactors by a precision syringe pump model 260 (World Precision Instrument, Sarasota, FL). Constant temperature in the microflow reactors during the experiments was maintained using heating plates connected to a temperature regulator (Philips, Kassel, Germany) and thermometer (Ahlborn, Holzkirchen, Germany) The whole instrumental setup for fluorescence imaging is schematically presented in Fig. S1 in the supplementary section.

3. Results and discussion

3.1. Probing hydrodynamic flow stability and segregation in the microflow reactor used

Here we present a microfluidic module for multi-step biomolecule selection in a cascadable (Fig. 1A). The microflow reactor is made by using two lithographic masks (Fig. 1B and C) etched at different depths. It consists of three inlet channels, a chamber with a bead barrier, and three outlet channels (Fig. 1D). The etched bead barrier restrained the 12 µm super-paramagnetic beads, delivered through the inlet channels, from leaving the bead chamber.

The spatially separated flow patterns in the standard transfer module (STM, see Fig. 1D), and the flow stability was tested using a fluorescence solution of 1 µM rhodamine 6G (R6G) while the microflow reactor was illuminated with an argon-ion laser. The fluorescence images were obtained by using tandem optics with a combination of

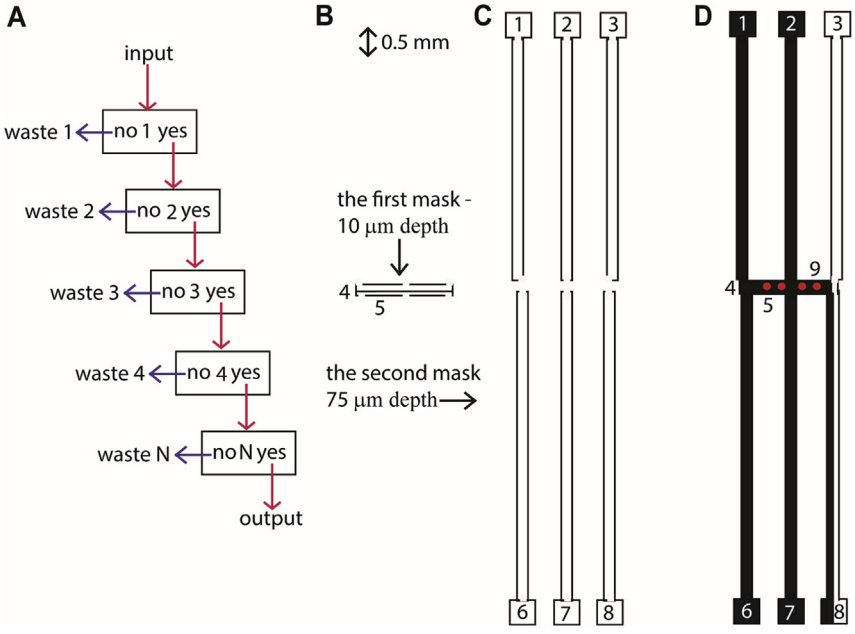

Fig. 1. DNA selection in microfluidics. (**A**) Multi-step biomolecule selection in cascadable connected modules. The input presents an initial pool of biomolecules, which undergoes N number selection steps. Certain molecules from the initial pool bind reversibly to a certain selection module when the selection condition is fulfilled. If not, the molecule is taken out of system. (**B**) A scheme of the first mask used to produce the microflow reactor. It is etched with a 10 µm depth for the chamber (5) and the bead barrier (4). (**c**) A scheme of the second mask introduces the inlet (1, 2, and 3) and the outlet (6, 7, and 9) channels and has a width of 180 µm and a depth of 75 µm. (**D**) The complete microflow reactor consists of three inlets (1, 2, and 3) and three outlets (6, 7, and 9) channels, a chamber (5) with beads (9) and a bead barrier (4) that restrains the bead, delivered from the inlets, from leaving the chamber through the outlets.

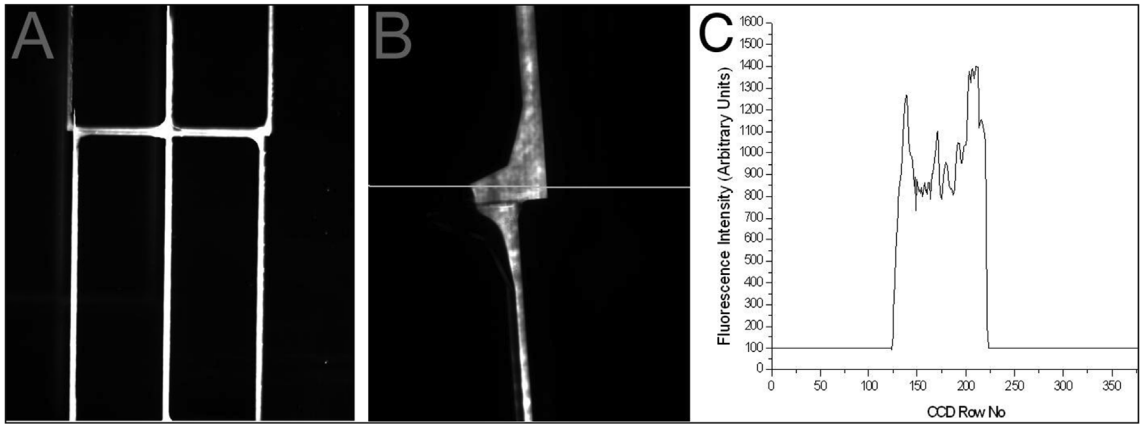

Fig. 2. Fluorescence images of steady flow patterns in a strand transfer module. (A) Tris solutions of rhodamine 6G were pumped through the three inlet channels on the top of the picture. The solution went out from the three outlet channels on the bottom of the picture. The exposure time was 1 s. (B) Tris solutions free of rhodamine 6G were pumped through the left-hand and the middle channel, while a sodium hydroxide solution containing rhodamine 6G was pumped through the right-hand channel. The flow rate on all channels was 0,5 μl/min. A quantix camera was used. The exposure time was half of a second. (C) The fluorescence intensity profile of the line from picture B is plotted.

fluorescence filters and a nitrogen-cooled CCD camera or a Quantrix CCD camera with a combination of a microscope, controlled by PMIS or ImageJ software. Firstly, the fluorescent solution of 1 μM rhodamine 6G, solved in a 500 mM Tris-acetate buffer solution and 50 mM NaOH was pumped through all inlet channels. The fluorescence images were obtained by using tandem optics with a combination of fluorescence filters and a nitrogen-cooled CCD (Fig. 2A).

Secondly, to prove the special segregation of the delivered solutions through different inlet channels a fluorescence solution of R6G, dissolved in 100 mM NaOH, was delivered through the channel 3, only, while non-fluorescence solutions of 1 M Tris were delivered via the middle channel 2 and a 500 mM Tris-acetate buffer solution and 50 mM NaOH via the channel 1. All solutions are delivered with a flow rate of 0.5 μl/min. The fluorescence images were obtained by using a Quantix CCD camera as described in the Material and Methods (Fig. S1). There is a sharp border between the non-fluorescent solution coming from the middle channel and the fluorescent solution coming from channel 3 (Fig. 2B and C). The result shows that a significant part on the right-hand side of the bead chamber contains a solution, which is coming from the channel 3 only. The microflow reactor's design is symmetric, which means that there is a similar part on the left-hand side of the chamber, through which the only solution from channel 1 is passing.

3.2. Automated DNA selection with movable magnetic beads and DNA hybridization kinetics and denaturation on microbeads in the microflow reactor used

To demonstrate DNA hybridization transfer the PVA super-paramagnetic beads were incorporated into the microchamber using the inlet channels (Fig. 3A and B). The DNA1 oligomer with a spacer of 14 dTs was immobilized to the bead (Fig. 3C) as described in Materials and Methods. The 14 dT-long spacer was used to avoid steric problems for DNA hybridization on a surface. Note that the beads are delivered via the inlet channels and are kept restrained in the chamber due to the bead barrier, which is smaller than the diameter of the beads.

A buffer solution of 500 mM Tris, pH 8.3, and 50 mM NaOH containing 1 μM, 5′-end R6G labeled DNA2 library in the concentration of 200 μM, assembled as described was delivered through the channel 1 while a 150 mM Tris, pH 8.3, solution through the middle and the right-hand channels with a flow rate of 0.5 μl/min. All beads were moved into the left-hand channel by a NdFeB block magnet (Fig. 3A). The fluorescence detection system with the Quantix CCD camera (Fig. S1) allowed us to measure a hybridization signal on a single bead of 224 AU (arbitrary units) shown in Fig. 3A. The 5′-end R6G labeled DNA2 library in a solution has a signal of 49 AU while the background signal of the microreactor was 15 AU (Fig. 3A). Next, a 150 mM Tris solution was delivered through all channels for 5 min at the same flow rate. Then the flow rate was stopped, and the beads were moved by the magnet into the right-hand channel within a few seconds. After that, a 150 mM Tris solution was delivered through chambers 1 and 2 while 100 mM NaOH was pumped through channel 3 at the same flow rate for 2 min. Next, fluorescence and white-light images from these beads were taken (Fig. 3B). The fluorescence signal on the beads (20 AU) has very close to the background signal (15 AU) due to DNA denaturation. A hybridization transfer of DNA was demonstrated, from channel 1 to channel 3, by moving beads 15 times, as the output flow was collected. The beads had a 50% magnetic content. Beads with a lesser magnetic content were impossible to be moved in the micro-reactor by the magnetic stand. We move the magnetic beads into microreactor by the magnetic stand under stop-flow conditions not only to facilitate the movement itself but also to avoid flow disturbance.

DNA hybridization and denaturation on beads under flow conditions are very rapid reactions. We demonstrate the speed of these reactions in the Video_file_1.mp4 under the same experimental conditions as described above. We have used the DNA1 oligomer immobilized to the same PVA beads, which this time was much more as they filled more of the inlet channel 1. We took fluorescence images from the beads incorporated into the microreactor with an interval of 1 s. From the first to the 10th second a hybridization buffer without DNA was delivered with a flow rate of 0.5 μl/min. The fluorescently labeled DNA library was delivered in the next 30 s as the fluorescent signal on the beads reached its maximum. In the next 2 s, we delivered a washing solution and after that denaturation solution of 100 mM NaOH. DNA denaturation from the beads is achieved within 2 s only. Note that the denaturation solution of 100 mM NaOH does not quench our fluorescent signal as already published (Penchovsky, 2013b).

Supplementary video related to this article can be found at https://doi.org/10.1016/j.bios.2019.04.014.

3.3. Probing specificity of DNA hybridization

We have already proven that we can perfectly well distinguish hybridization between perfectly matching oligonucleotides and these with 2-mismatches over a length of 21 nt in the applied by us buffers for *DNA hybridization transfer* under isothermal conditions (Penchovsky, 2013b). In addition, we have also ready proven that we can perfectly well distinguish hybridization between perfectly matching oligonucleotides and these with 2-mismatches over a length of 21 nt on beads applying a

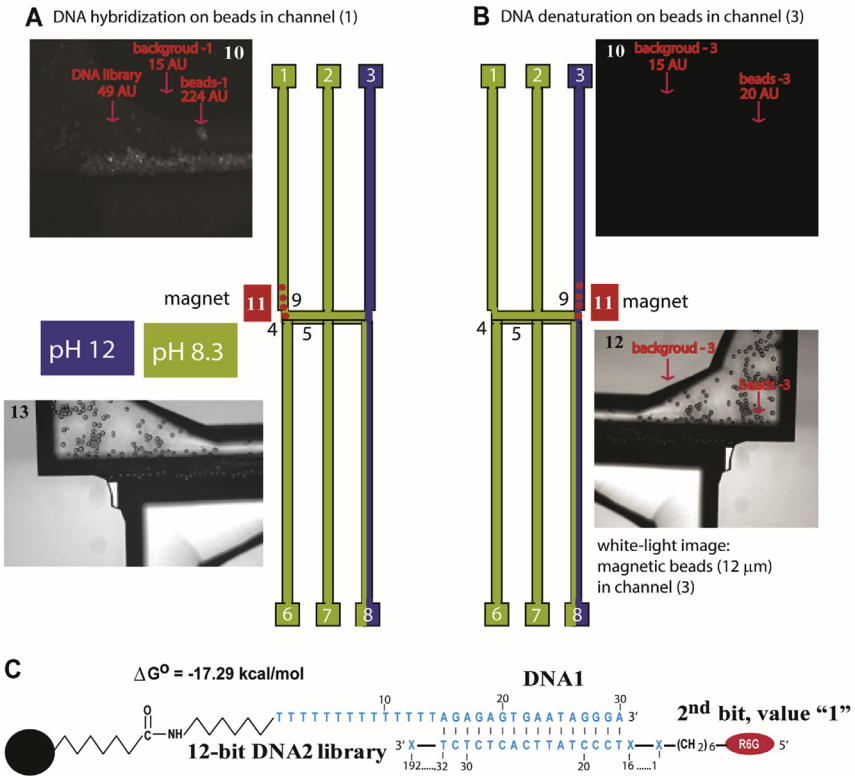

Fig. 3. An automated DNA selection in a microchamber using movable magnetic beads. (**A**) Tris-solution, free of R6G, is pumped through the left-hand (1) and the middle (2) channel while a sodium hydroxide solution containing R6G was pumped through the channel 3 of the microflow reactor (Fig. 1c). The solutions flow out through the outlets (6, 7, and 8). A fluorescence image of the channel 3 with a part of the chamber (5) filled with beads (9) that are restricted into the chamber by a bead barrier (4) with intensity profile is shown in a picture (10). (**B**) A solution of the 5′-end-R6G labeled DNA library is pumped through the channel (1). A 150 mM Tris, pH 8.3 solution is pumped through the middle channel (2) and a 100 mM NaOH solution - through the channel (3). All beads (9) with immobilized DNA (see C) are fixed in the left-hand corner of the bead chamber (5) by a magnet (11). As a result, the DNA hybridization on the 12 µm PVA super-paramagnetic beads takes place because the pH of this part of the chamber is 8.3 units. The fluorescence image is shown in the picture (10). The beads (9) were moved by the magnet (11) into the right-hand corner of the microreactor chamber (5). DNA hybridized to the beads was denatured with a 100 mM NaOH solution flowing through the channel (3). A fluorescence image obtained from the beads (10) and a white light image on the pictures (12, 13). (**C**) A 30mer DNA6 with immobilized to PVA super-paramagnetic beads. A solution of 5′-end —R6G labeled DNA library hybridized to the DNA on the beads at the 9th with a value '0'. It is 12-bit DNA library that has 4096 different DNA strands each 192 nt long. Each bit is 16 nt long.

washing step (Penchovsky and McCaskill, 2002).

Here we demonstrate that we can perfectly well distinguish hybridization between perfectly matching oligonucleotides and these with 5-mismatches over a length of 21 nt (Fig. S2). One DNA strand is immobilized on the beads while the other is fluorescently-labeled. The beads are placed in the microflow reactor. In this case, we prove no washing step is needed to make distinguish hybridization between perfectly matching oligonucleotides and these with 5-mismatches over a length of 21 nt. After saturation of DNA hybridization on beads placed in the microflow reactor the fluorescent signal of perfectly matching DNA oligomers is about 1700 AU (Figs. S3A and C). In contrast, the fluorescent signal of hybridization between the oligomers with 5 mismatches is 700 AU (Figs. S3B and C), which is close to the fluorescent signal in the solution (200 AU) plus the bias signal of the camera (500 AU). After removing the fluorescent solution without any further washing steps, the fluorescent signal of perfectly matching oligomers is down with about 200 AU (Figs. S4A and C) while the signal of the mismatching oligomers is down to the bias signal of the camera (Figs. S4B and C).

3.4. Probing specificity of DNA hybridization transfer in the microflow reactor by PCR

The DNA2 is a 12-bit DNA library that encodes binary information into single-stranded DNA molecules (either "0", or "1"). Each strand, 5′-end R6G labeled, is 192 nt long and has 12 bits, as each bit is 16 nt long (Fig. 4A). The whole library has 4096 different strands (Penchovsky and Ackermann, 2003). The DNA library was proven to amplify with all antisense bits/primers with high fidelity under uniform conditions (Penchovsky and Ackermann, 2003).

The output flow solution of channel 3 was collected during the experiment described in the previous section (3.2) and was precipitated, deposited, and finally dissolved in the 50 µl stirrer water. We used 1 µl of this solution to perform two PCR readouts with primers either for the 2nd bit with a value "0" or for the 2nd bit with value "0" under conditions described in Materials and Methods (Fig. 4B). Only the readout with the primer 2nd bit with value"0" gave a signal with a length of 44 bp (Fig. 4C). These results suggest that the automated DNA hybridization transfer in our microreactor was performed with a high-level of specificity under the established protocol.

4. Discussion

The first idea was to implement the automated DNA selection procedure by moving magnetic beads in STMs under steady-flow conditions without altering the solutions (McCaskill et al., 2001). This was proven practically not feasible due to two obstacles. The first obstacle was related to the very difficult bead movement into the chamber of the microreactor by a magnetic stand. The second problem was to preserve the flow segregation between the hybridization buffer and denaturation solution into the chamber under steady-flow conditions during the bead movement. To overcome these problems we applied beads with 50% magnetic content, very strong magnetic stands and performed the DNA selection under stop-flow conditions with altering solutions. It was possible to move the beads from one corner to other into microchamber under stop-flow conditions within 2 s in contrast to steady-flow where the moving beads against the current flow were very much problematic. In addition, we use a reciprocation between the hybridization buffer and the denaturation the solutions delivered via the first inlet channel. We moved the beads from the left-hand (hybridization) corner of the chamber to the right-hand (denaturation) corner while applying a washing solution via the hybridization channel and under stop-flow condition. This solved not only the problem with the bead movement but also excluded any possibility of contamination of the denaturing solution with DNA from the hybridization buffer during the bead movement into the denaturing corner. Because of this, we adopted the DNA hybridization transfer under stop-flow conditions in adjunction with reciprocation between the hybridization buffer and the denaturation the solutions delivered via the first inlet channel. This made the DNA hybridization transfer by moving magnetic beads in the microreactor not only possible but also very accurate as confirmed by our PCR experiments.

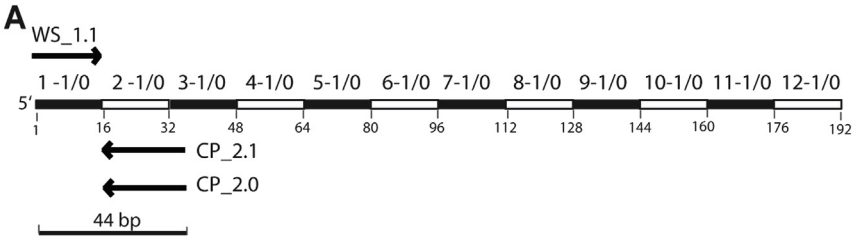

B

N	Bits	5'-3' Word sequences 16 nt	5'-3' Capture probe sequences 28 nt
1	1.1	CCATCACTACCTTCAT	TTTTTTTTTTTTATGAAGGTAGTGATGG
2	1.0	TCCTCTATCATCCTCA	TTTTTTTTTTTTTGAGGATGATAGAGGA
3	2.1	TCCCTATTCACTCTCT	TTTTTTTTTTTTAGAGAGTGAATAGGGA
4	2.0	CACACCTCAACTTCTT	TTTTTTTTTTTTAAGAAGTTGAGGTGTG

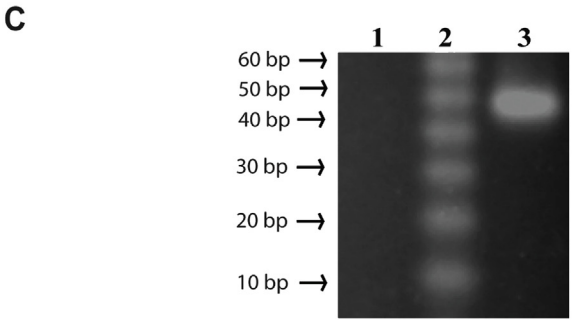

Fig. 4. A PCR detection of an automated DNA selection in a microchamber using movable magnetic beads. (**A**) A schematic presentation of a 12-bit DNA library used for DNA selection. (**B**) The sequences of the first and the second bits of the DNA library with values "1" and "0" used as primers. (**C**) An image of 4% agarose gel shows the PCR amplification of the selected DNA in the micro flow reactor, where start 1 with a PCR product obtained with primers 1.1 and 2.0; start 2 is loaded with a 10bp step ladder dsDNA (Promega Corporation, Madison, WI, USA); start 2 with a PCR product obtained with primers 1.1 and 2.1.

This automated DNA selection by moving magnetic beads into microreactors can apply an already published chemical procedure for multiple DNA hybridization and selection under isothermal conditions in microchambers connected in a cascade. This chemical procedure employed reversible pH-alterations of the solutions used and implement multistep selection based on DNA hybridization/denaturation on beads in cascade microchambers (Penchovsky and McCaskill, 2002) (Penchovsky, 2013b). Moreover, we can implement immobilization of different DNA oligomers to beads placed in cascade microchambers using already published pH-dependent (Penchovsky, 2013b) or UV-dependent chemical procedures (Penchovsky et al., 2000). Therefore, we can regard the presented approach for automated DNA selection procedure by moving magnetic beads in STMs as an element that can be integrated into complex microfluidic platforms. If we use magnetic beads with a capacity high-density DNA immobilization we can also easily perform a solid-state PCR under isothermal conditions.

5. Conclusions

The presented method takes advantage of the fast DNA hybridization under flow conditions by reaching saturation within 30 s, the instant DNA denaturation with 2 s, and small working volumes with a microliter scale. In addition, the method is fully automated and can detect DNA hybridization a single microbead that makes it extremely sensitive within femtograms for 50mer DNA oligomers. Moreover, it was proven a high-level DNA hybridization on beads under hybridization solutions used. After applying a washing step we were able to distinguish between perfect matches and 2 mismatches over 24bp DNA oligomer as already published elsewhere (Penchovsky and McCaskill, 2002) (Penchovsky, 2013b). All these features make the proposed methods very suitable for building complex and integrated microfluidic devices in fields of fully automated DNA selection, detection, and amplification.

Competing interests

The author declares no competing financial interest.

Acknowledgments

This research is funded by Fraunhofer-Gesellschaft, Germany and by a grant DN13/14/20.11.2017 awarded by the Bulgarian National Science Fund.

Appendix A. Supplementary data

Supplementary data to this article can be found online at https://doi.org/10.1016/j.bios.2019.04.014.

References

Blount, K., Puskarz, I., Penchovsky, R., Breaker, R., 2006. Development and application of a high-throughput assay for glmS riboswitch activators. RNA Biol. 3 (2), 77–81.
McCaskill, J.S., Penchovsky, R., Gohlke, M., Ackermann, J., T, R., 2001. Steady flow micro-reactor module for pipelined DNA computations. Lect. Notes Comput. Sci. 2054, 263–270.
Na, W., Nam, D., Lee, H., Shin, S., 2018. Rapid molecular diagnosis of infectious viruses in microfluidics using DNA hydrogel formation. Biosens. Bioelectron. 108, 9–13.
Olcer, Z., Esen, E., Ersoy, A., Budak, S., Sever Kaya, D., Yagmur Gok, M., Barut, S., Ustek, D., Uludag, Y., 2015. Microfluidics and nanoparticles based amperometric biosensor for the detection of cyanobacteria (Planktothrix agardhii NIVA-CYA 116) DNA. Biosens. Bioelectron. 70, 426–432.
Pekin, D., Taly, V., 2017. Droplet-based microfluidics digital PCR for the detection of KRAS mutations. Methods Mol. Biol. 1547, 143–164.
Penchovsky, R., 2012. Engineering integrated digital circuits with allosteric ribozymes for scaling up molecular computation and diagnostics. ACS Synth. Biol. 1 (10), 471–482.
Penchovsky, R., 2013a. Computational design and biosensor applications of small molecule-sensing allosteric ribozymes. Biomacromolecules 14 (4), 1240–1249.
Penchovsky, R., 2013b. Programmable and automated bead-based microfluidics for versatile DNA microarrays under isothermal conditions. Lab Chip 13 (12), 2370–2380.
Penchovsky, R., 2014. Computational design of allosteric ribozymes as molecular biosensors. Biotechnol. Adv. 32 (5), 1015–1027.
Penchovsky, R., Ackermann, J., 2003. DNA library design for molecular computation. J. Comput. Biol. 10 (2), 215–229.
Penchovsky, R., Birch-Hirschfeld, E., McCaskill, J.S., 2000. End-specific covalent photo-

dependent immobilisation of synthetic DNA to paramagnetic beads. Nucleic Acids Res. 28 (22), E98.
Penchovsky, R., Breaker, R.R., 2005. Computational design and experimental validation of oligonucleotide-sensing allosteric ribozymes. Nat. Biotechnol. 23 (11), 1424–1433.
Penchovsky, R., McCaskill, J.S., 2002. Cascadable hybridisation transfer of specific DNA between microreactor selection modules. Lect. Notes Comput. Sci. 2340, 46–56.
Penchovsky, R., Stoilova, C.C., 2013. Riboswitch-based antibacterial drug discovery using high-throughput screening methods. Expert Opin. Drug Discov. 8 (1), 65–82.
Penchovsky, R., Traykovska, M., 2015. Designing drugs that overcome antibacterial resistance: where do we stand and what should we do? Expert Opin. Drug Discov. 10 (6), 631–650.
Shamsi, M.H., Choi, K., Ng, A.H., Chamberlain, M.D., Wheeler, A.R., 2016. Electrochemiluminescence on digital microfluidics for microRNA analysis. Biosens. Bioelectron. 77, 845–852.
Yan, Y., Boey, D., Ng, L.T., Gruber, J., Bettiol, A., Thakor, N.V., Chen, C.H., 2016. Continuous-flow C. elegans fluorescence expression analysis with real-time image processing through microfluidics. Biosens. Bioelectron. 77, 428–434.
Yu, T., Tang, C., Zhang, Y., Zhang, R., Yan, W., 2017. Microfluidics-based digital quantitative PCR for single-cell small RNA quantification. Biol. Reprod. 97 (3), 490–496.
Zhao, L., Ma, C., Shen, S., Tian, C., Xu, J., Tu, Q., Li, T., Wang, Y., Wang, J., 2016. Pneumatic microfluidics-based multiplex single-cell array. Biosens. Bioelectron. 78, 423–430.